PROCEEDINGS OF SCIENCE

Searches for heavy diboson resonances in semi–leptonic final states in pp collisions at 13 TeV with the ATLAS detector

Zhongyukun XU[a,b,*]

[a] *Shandong University*
72 Bihai Road, Jimo, Qingdao, China
[b] *Department of Physics, University of Michigan*
500 S. State Street, Ann Arbor, USA

E-mail: zhongyukun.xu@cern.ch

A search for heavy resonances decaying into WW, ZZ or WZ is performed, using proton–proton collision data at a centre-of-mass energy of $\sqrt{s}$ = 13 TeV. The data, corresponding to an integrated luminosity of 139 fb^{-1}, were recorded with the ATLAS detector from 2015 to 2018 at the Large Hadron Collider. The search is performed for final states in which one W or Z boson decays leptonically, and the other W boson or Z boson decays hadronically. The data are found to be described well by expected backgrounds. Upper bounds on the production cross sections of heavy resonances are derived in the mass range 300–5000 GeV within the context of Standard Model extensions with a neutral scalar, a heavy vector triplet or warped extra dimensions. Production through gluon–gluon fusion, Drell–Yan or vector-boson fusion are considered, depending on the assumed model.

The Eighth Annual Conference on Large Hadron Collider Physics-LHCP2020
25-30 May, 2020
online

[*] Speaker

PoS(LHCP2020)217

1. Introduction

Many BSM models like the two-Higgs-doublet model [1], composite Higgs models [2, 3], technicolour [4, 5, 6] models, and warped extra dimensions [7, 8] predict the existence of heavy resonances decay into vector boson pairs. On the Large Hadron Collider (LHC). This search focuses on diboson resonance produced by through gluon–gluon fusion (ggF), Drell–Yan (DY), or vector-boson fusion (VBF) processes figure1 and decaying into Semileptonic VV final states which one vector boson decays leptonically (V_ℓ: $W \to \ell\nu$, $Z \to \ell\ell$ or $Z \to \nu\nu$) while the other decays hadronically (V_h: $V \to qq$). The hadronic $V \to qq$ decays can result in either two separate small-radius jets (small-R jet, or j) or as one large-radius jet (large-R jet, or J) depending on the transverse momentum (p_{T}) of the boson. The further details can be find in the paper [9].

2. Signal and background

Monte Carlo (MC) simulations were used for background modellings and estimations, evaluations of signal efficiencies, optimisations of event selections, and estimations of systematic uncertainties. Three different models corresponding to different spins are considered in this searches. The first one is a scalar neutral radion, introduced in some bulk RS models to stabilise the radius of the compactified extra dimension r_c [10, 11]. The second type considered comprises two heavy vector bosons described in the HVT framework [12]: an electrically charged W' boson and an electrically neutral Z' boson produced through the DY and VBF processes. The third benchmark resonance searched for is a spin-2 bulk RS graviton G_{KK} which appears as the first KK excitation of the gravitational field in a bulk RS graviton model [7, 13, 14].

The most background comes from processes having similar final states which are hard to distinguish or easy to mis-identify, including W and Z boson production in association with jets (W+jets and Z+jets), top-quark production (both top-quark pair, , and single-top-quark), non-resonant diboson production (WW, WZ and ZZ), and multijet production. MC samples were produced to model these background processes with the exception of multijet production, for which data were used to estimate its contribution. Multijet contribution is estimated by template method using multijet enriched control regions.

3. Object reconstruction and identification

The study focus on leptons, jets, and $E_{\mathrm{T}}^{\mathrm{miss}}$. For leptons, only electron and muon are considered in this search. The neutrino in the final state results in a large missing transverse momentum. For jets, small-R jets and large-R jets are considered to face different decay scenarios. Electrons are reconstructed from energy clusters that are consistent with EM showers in the ECAL and are matched to tracks in the ID. They are required to have transverse energy $E_{\mathrm{T}} > 7$ GeV and pseudorapidity $|\eta| < 2.47$, excluding the ECAL barrel–endcap transition region: $1.37 < |\eta| < 1.52$. Muons are identified by matching MS tracks with those in the ID and are required to have transverse momentum $p_{\mathrm{T}} > 7$ GeV and pseudorapidity $|\eta| < 2.5$. Both electron and muon require to have $p_{\mathrm{T}} > 30$ GeV and pass the corresponding isolation requirement. Details can be found in Refs. [15, 16].

Small-R jets are reconstrued by using anti-k_t algorithm [17, 18] with a radius parameter of $R = 0.4$ with the extra requirement of $p_{\mathrm{T}} > 30$ GeV and $|\eta| < 4.5$. The jet vertex tagger [19] is

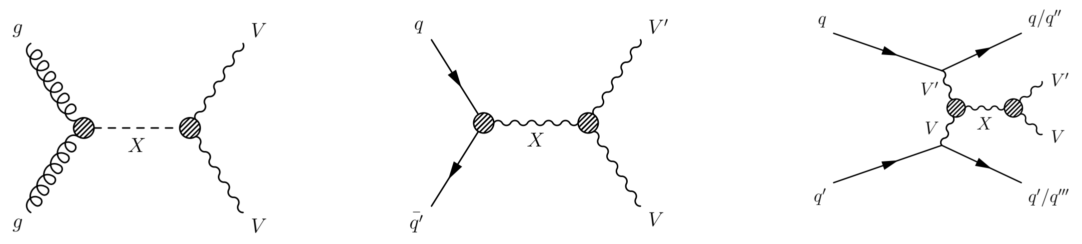

(a) gluon–gluon fusion **(b)** Drell–Yan **(c)** vector-boson fusion

Figure 1: The Feynman diagrams explaining the production of heavy resonances X with their decays into a pair of vector bosons. The hashed circles represent direct or effective couplings.

applied to Jet with $p_{\mathrm{T}} < 120$ GeV and $|\eta| < 2.5$ to suppress pile-up effect. For identification of small-R jets containing b-hadrons (b-tagging), a multivariate algorithm [20] is used. Due to ID coverage, only $|\eta| < 2.5$ jets are tagged. The effciency of b-tagging algorithm is 85% according to simulated test. Large-R jets are reconstructed from track-calo clusters [21] with the anti-k_t algorithm, but with the radius parameter increased to $R = 1.0$.The large-R jets are required to have $p_{\mathrm{T}} > 200$ GeV, $|\eta| < 2.0$, and a jet mass (m_J) greater than 50 GeV. Variable-radius (VR) jets are used to identify b-jets from boosted hadronic $V \rightarrow qq$ decays that are reconstructed as large-R jets, which details can be see in public note [22].

The missing transverse momentum ($\vec{E}_{\mathrm{T}}^{\mathrm{miss}}$) is calculated as the negative vectorial sum of the transverse momenta of calibrated electrons, muons, small-R jets, and unassociated tracks. Large-R jets are not included in the $\vec{E}_{\mathrm{T}}^{\mathrm{miss}}$ calculation to avoid double-counting of energy between the small-R jets and large-R jets. Details can be found in the publication [23].

4. Event Selection

The search selection begins with leptonically decay boson V_l. Events are selected with certain p_{T} and $E_{\mathrm{T}}^{\mathrm{miss}}$ requirement lepton number and categorized into 0/1/2 lepton channel while extra lepton events veto. Though the selection requirement differs between different channels, the selection flows are the same. All channel then go through the hadronically decay boson selection, which requires one large-R jets or two small-R jets with η and p_{T} requirement. Events are further categorized into b-tagged/untagged by whether two VR(small-R) jets pass b-tagging requirement. Last, a cleaning cut based ratio between $p_{\mathrm{T}}^{V_h}$ and $m_V V$ is applied for extra QCD background rejection.

A mass windows cut on V_h with different requirement between merged and resolved analysis is used to define signal region (SR). The merged analysis uses p_{T} dependent mass window cut while resolved analysis uses a fixed mass window cut. Two kind of CRs are selected to estimate different background modeling. The mass window sideband regions are selected as W+jets and Z+jets control region for its enriched W+jets and Z+jets contribution and simliar kinematics with SRs.

Top control region requires extra b-tagged besides the V_h decay jets as Top quark large branch ratio decaying to jets containing b-hadron.

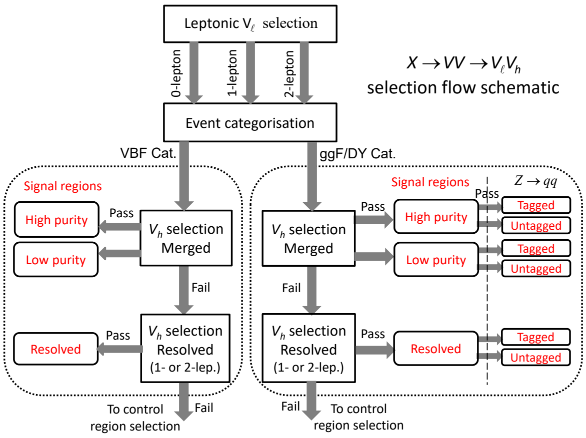

Figure 2: Illustration of the selection flow and signal regions of the $X \to VV \to V_\ell V_h$ search.

5. Result

The statistical analysis is based on the framework described in Refs. [24, 25, 26]. Maximum-likelihood fits are made to the observed binned distributions of the final discriminants in SRs, m_{T} in 0-lepton, $m_{\ell\nu J}$ or $m_{\ell\nu jj}$ in 1-lepton and $m_{\ell\ell J}$ or $m_{\ell\ell jj}$ in 2-lepton, and to the numbers of observed events in CRs simultaneously. The mass ranges fitted are 300–3000 GeV for the resolved analysis and 500–6000 GeV for the merged analysis. No significant excess is found in the post-fit distribution, so a limit setting with 95% CLs are made.

Table 1 summarises the observed and expected 95% confidence level (CL) lower limits on the masses of the resonances in the benchmark models studied in this paper. These mass limits and the cross-section upper limits presented above are significantly more stringent than those published previously. Compared to the searches with the 36.1 fb^{-1} data set in the same leptonic final states [27, 28], an improvement of a factor of three or more in the cross-section upper limits is obtained for most of the searches at the highest masses.

Table 1: Observed (expected) 95% CL lower limits on the mass, in TeV, of different resonances in the benchmark models studied. The symbol "–" means no limit is set.

Production process	RS radion	HVT			RS graviton
			W'	Z'	
ggF/DY	3.2 (2.9)	Model A	3.9 (3.8)	3.5 (3.4)	2.0 (2.2)
		Model B	4.3 (4.0)	3.9 (3.7)	
VBF	–	Model C	–	–	0.76 (0.77)

References

[1] G. C. Branco et al. "Theory and phenomenology of two-Higgs-doublet models". In: *Phys. Rept.* 516 (2012), pp. 1–102. DOI: 10.1016/j.physrep.2012.02.002. arXiv: 1106.0034 [hep-ph].

[2] Michael J. Dugan, Howard Georgi, and David B. Kaplan. "Anatomy of a Composite Higgs Model". In: *Nucl. Phys. B* 254 (1985), pp. 299–326. DOI: 10.1016/0550-3213(85)90221-4.

[3] Kaustubh Agashe, Roberto Contino, and Alex Pomarol. "The Minimal composite Higgs model". In: *Nucl. Phys. B* 719 (2005), pp. 165–187. DOI: 10.1016/j.nuclphysb.2005.04.035. arXiv: hep-ph/0412089 [hep-ph].

[4] Estia Eichten and Kenneth Lane. "Low-scale technicolor at the Tevatron and LHC". In: *Phys. Lett. B* 669 (2008), pp. 235–238. DOI: 10.1016/j.physletb.2008.09.047. arXiv: 0706.2339 [hep-ph].

[5] Simon Catterall et al. "MCRG Minimal Walking Technicolor". In: *Phys. Rev. D* 85 (2012), p. 094501. DOI: 10.1103/PhysRevD.85.094501. arXiv: 1108.3794 [hep-ph].

[6] J. R. Andersen et al. "Discovering Technicolor". In: *Eur. Phys. J. Plus* 126 (2011), p. 81. DOI: 10.1140/epjp/i2011-11081-1. arXiv: 1104.1255 [hep-ph].

[7] Lisa Randall and Raman Sundrum. "A Large Mass Hierarchy from a Small Extra Dimension". In: *Phys. Rev. Lett.* 83 (1999), pp. 3370–3373. DOI: 10.1103/PhysRevLett.83.3370. arXiv: hep-ph/9905221 [hep-ph].

[8] H. Davoudiasl, J. L. Hewett, and T. G. Rizzo. "Bulk gauge fields in the Randall-Sundrum model". In: *Phys. Lett. B* 473 (2000), pp. 43–49. DOI: 10.1016/S0370-2693(99)01430-6. arXiv: hep-ph/9911262 [hep-ph].

[9] ATLAS Collaboration. *Search for heavy diboson resonances in semileptonic final states in pp collisions at $\sqrt{s}$ = 13 TeV with the ATLAS detector*. CERN-EP-2020-049. 2020. URL: https://cds.cern.ch/record/2716405.

[10] Walter D. Goldberger and Mark B. Wise. "Modulus Stabilization with Bulk Fields". In: *Phys. Rev. Lett.* 83 (1999), pp. 4922–4925. DOI: 10.1103/PhysRevLett.83.4922. arXiv: hep-ph/9907447 [hep-ph].

[11] Walter D. Goldberger and Mark B. Wise. "Phenomenology of a stabilized modulus". In: *Phys. Lett. B* 475 (2000), pp. 275–279. DOI: 10.1016/S0370-2693(00)00099-X. arXiv: hep-ph/9911457 [hep-ph].

[12] Duccio Pappadopulo et al. "Heavy vector triplets: bridging theory and data". In: *JHEP* 09 (2014), p. 060. DOI: 10.1007/JHEP09(2014)060. arXiv: 1402.4431 [hep-ph].

[13] Tao Han, Joseph D. Lykken, and Ren-Jie Zhang. "On Kaluza-Klein states from large extra dimensions". In: *Phys. Rev. D* 59 (1999), p. 105006. DOI: 10.1103/PhysRevD.59.105006. arXiv: hep-ph/9811350 [hep-ph].

PoS(LHCP2020)217

[14] Kaustubh Agashe et al. "Warped gravitons at the LHC and beyond". In: *Phys. Rev. D* 76 (2007), p. 036006. DOI: 10.1103/PhysRevD.76.036006. arXiv: hep-ph/0701186 [hep-ph].

[15] ATLAS Collaboration. "Electron and photon performance measurements with the ATLAS detector using the 2015–2017 LHC proton–proton collision data". In: *JINST* 14 (2019), P12006. DOI: 10.1088/1748-0221/14/12/P12006. arXiv: 1908.00005 [hep-ex].

[16] ATLAS Collaboration. "Muon reconstruction performance of the ATLAS detector in proton–proton collision data at $\sqrt{s}$ = 13 TeV". In: *Eur. Phys. J. C* 76 (2016), p. 292. DOI: 10.1140/epjc/s10052-016-4120-y. arXiv: 1603.05598 [hep-ex].

[17] Matteo Cacciari, Gavin P. Salam, and Gregory Soyez. "The anti-k_t jet clustering algorithm". In: *JHEP* 04 (2008), p. 063. DOI: 10.1088/1126-6708/2008/04/063. arXiv: 0802.1189 [hep-ph].

[18] Matteo Cacciari, Gavin P. Salam, and Gregory Soyez. "FastJet user manual". In: *Eur. Phys. J. C* 72 (2012), p. 1896. DOI: 10.1140/epjc/s10052-012-1896-2. arXiv: 1111.6097 [hep-ph].

[19] ATLAS Collaboration. *Tagging and suppression of pileup jets with the ATLAS detector*. ATLAS-CONF-2014-018. 2014. URL: https://cds.cern.ch/record/1700870.

[20] ATLAS Collaboration. "ATLAS b-jet identification performance and efficiency measurement with $t\bar{t}$ events in pp collisions at $\sqrt{s}$ = 13 TeV". In: *Eur. Phys. J. C* 79 (2019), p. 970. DOI: 10.1140/epjc/s10052-019-7450-8. arXiv: 1907.05120 [hep-ex].

[21] ATLAS Collaboration. *Improving jet substructure performance in ATLAS using Track-CaloClusters*. ATL-PHYS-PUB-2017-015. 2017. URL: https://cds.cern.ch/record/2275636.

[22] ATLAS Collaboration. *Variable Radius, Exclusive-k_T, and Center-of-Mass Subjet Reconstruction for Higgs($\rightarrow b\bar{b}$) Tagging in ATLAS*. ATL-PHYS-PUB-2017-010. 2017. URL: https://cds.cern.ch/record/2268678.

[23] ATLAS Collaboration. "Performance of missing transverse momentum reconstruction with the ATLAS detector using proton–proton collisions at $\sqrt{s}$ = 13 TeV". In: *Eur. Phys. J. C* 78 (2018), p. 903. DOI: 10.1140/epjc/s10052-018-6288-9. arXiv: 1802.08168 [hep-ex].

[24] ATLAS Collaboration. "Combined search for the Standard Model Higgs boson in pp collisions at $\sqrt{s}$ = 7 TeV with the ATLAS detector". In: *Phys. Rev. D* 86 (2012), p. 032003. DOI: 10.1103/PhysRevD.86.032003. arXiv: 1207.0319 [hep-ex].

[25] Lorenzo Moneta et al. "The RooStats Project". In: *PoS* ACAT2010 (2010), p. 057. DOI: 10.22323/1.093.0057. arXiv: 1009.1003 [physics.data-an].

[26] Wouter Verkerke and David P. Kirkby. "The RooFit toolkit for data modeling". In: *eConf* C0303241 (2003), MOLT007. arXiv: physics/0306116 [physics].

[27] ATLAS Collaboration. “Search for WW/WZ resonance production in $\ell\nu qq$ final states in pp collisions at $\sqrt{s}$ = 13 TeV with the ATLAS detector”. In: *JHEP* 03 (2018), p. 042. DOI: 10.1007/JHEP03(2018)042. arXiv: 1710.07235 [hep-ex].

[28] ATLAS Collaboration. “Searches for heavy ZZ and ZW resonances in the $\ell\ell qq$ and $\nu\nu qq$ final states in pp collisions at $\sqrt{s}$ = 13 TeV with the ATLAS detector”. In: *JHEP* 03 (2018), p. 009. DOI: 10.1007/JHEP03(2018)009. arXiv: 1708.09638 [hep-ex].